Respiratory motion correction for quantitative PET/CT using all detected events with internal—external motion correlation

Chi Liu[a)]
Department of Diagnostic Radiology, Yale University, New Haven, Connecticut 06520

Adam M. Alessio and Paul E. Kinahan
Department of Radiology, University of Washington, Seattle, Washington 98195

(Received 27 October 2010; revised 5 April 2011; accepted for publication 5 April 2011; published 9 May 2011)

Purpose: We present a method to correct respiratory motion blurring in PET/CT imaging using internal–external (INTEX) motion correlation. The internal motion of a known tumor is derived from respiratory-gated PET images; this internal motion is then correlated with external respiratory signals to determine the complete information of tumor motion during the scan.
Methods: For each PET/CT data, PET listmode data were phase-gated into five bins and reconstructed. The centroid of a targeted tumor in each bin was determined and correlated with the corresponding mean displacement of externally monitored respiratory motion signal. Based on this correlation, the external motion signal was converted into internal tumor motion information in the superior–inferior direction. Then, the PET listmode data were binned sequentially to multiple 1-s sinograms. According to the converted internal tumor motion signal, each 1-s sinogram was registered to a reference frame, which best matched the helical CT attenuation map based on consistency conditions. The registered sinograms were summed and reconstructed to form an image, corrected for the motion of the specific tumor. In this study, the proposed INTEX method was evaluated with phantom and patient studies in terms of tracer concentration and volume.
Results: The INTEX method effectively recovered the tracer concentration to the level of the stationary scan data in the phantom experiment. In the patient study, the INTEX method yielded a $(17 \pm 22)\%$ tumor volume decrease and a $(10 \pm 10)\%$ tumor SUVmax increase compared to nongated images.
Conclusions: The proposed INTEX method reduces respiratory motion degradation of PET tumor quantification and delineation in an effective manner. This can be used to improve the assessment of response to therapy for a known tumor by minimizing residual motion and matching the attenuation correction, without increasing image noise. [DOI: 10.1118/1.3582692]

Key words: respiratory motion correction, PET/CT, internal-external motion correlation

I. INTRODUCTION

PET/CT has become an important tool to assess the response to therapy for cancer patients.[1] However, respiratory motion can have a major degrading impact on PET-based tumor quantification and delineation.[2–5] For clinically relevant tumor sizes and motion, our previous study showed that respiratory motion can lead to a tracer concentration underestimation of 30% or more, and overestimation of tumor volume by a factor of two or more.[6]

To correct for respiratory motion, the most widely used method is respiratory-gated PET/CT, which divides PET data into different gates based on either temporal phase or respiratory displacement information with potential 4D CT for phase-matched attenuation correction.[7–17] However, since each gated image contains only a fraction of the detected coincidence events, the increased image noise can lead to substantial overestimation of tracer concentration measured by maximum standardized uptake value (SUVmax). Our previous study showed that for typical phase gating schemes, increased noise could cause a 9% tumor SUVmax overestimation on average.[18]

Another category of motion correction methods utilizes all the detected coincident events, leading to no increase in image noise compared to the static ungated PET image. These methods typically start with respiratory-gated PET or CT data and incorporate estimated image-based motion vectors either into the image reconstruction[19–24] or postprocessing.[25–27] The image-based motion vector used in these methods can be derived either from respiratory-gated PET or CT images. If estimated from gated PET images, the motion vectors are subject to the high levels of image noise, and the estimation errors can propagate into the motion-corrected images. On the other hand, gated CT images have much lower noise and can potentially generate more accurate motion vectors, but the patient motion during CT acquisition can be very different from the motion during PET acquisition because of respiration variations.[28] In addition, these approaches may require nonrigid volumetric image registration, which is sensitive to numerous free parameters and typically does not preserve PET tracer concentration.

Alternatives to gating are breath-hold PET/CT methods, which require patients to hold their breath repeatedly

during the PET and/or CT acquisition.[5,29–31] The breath-hold PET/CT images have the potential for less respiratory motion-blurring effects and more accurately aligned PET/CT images. However, this method is difficult to universally apply, as 40%–60% patients with lung cancer are unable to tolerate breath holding.[32]

The ideal motion correction method for PET tumor quantification would be able to effectively correct for respiratory motion with matched attenuation correction and use all the detected events so that the image noise in the corrected image is the same as the ungated static PET image. This leads to our proposed INTEX method, which aims to provide accurate PET tumor quantification and delineation for evaluating the response to therapy. It should be noted that the INTEX method is not designed for tumor detection tasks but for tumor quantification, as this method requires tracking the motion of known lesions. The first step of this method is establishing a correlation between external chest/abdomen motion, which can be tracked with high fidelity and temporal resolution, and internal tumor motion, which is generally more difficult to track. The high fidelity external motion is converted to the internal tumor motion according to this correlation. Then, based on this internal tumor motion information, we correct for respiratory motion with a full utilization of all the detected events.

II. METHODS

II.A. Phantom data sets

A Data Spectrum® anthropomorphic cardiac-torso phantom including lungs and liver was used to acquire experimental data. A total activity of ~10 mCi F-FDG at the start time of acquisition was injected into the phantom. The activity ratios for liver: background: lungs were 25:5:1. Two spherical "lesions" were inserted into the lung and liver, respectively. The lung lesion had an inner diameter of ~1.1 cm and the liver lesion had an inner diameter of ~1.4 cm. The lesion-to-lung ratio for the lung lesion and the lesion-to-liver ratio for the liver lesion were both 8:1. The phantom was positioned on the QUASAR® programmable respiratory motion platform from Modus Medical Devices Inc. (London, Ontario, Canada). The phantom data were acquired on a General Electric (GE) DSTE PET/CT scanner (Waukesha, WI) operated in 2D mode with one bed position. We first scanned the stationary phantom without motion and then scanned the moving phantom driven by the QUASAR® platform. We used a regular patient respiratory trace to generate two new traces, with mean motion amplitudes across all the cycles scaled to 16 and 11 mm. We used them to drive the QUASAR® platform to translate the phantom during scanning (shown in Fig. 1). The phantom motion was monitored and recorded by the Real-time Positioning Management (RPM) gating system (Varian, Palo Alto, CA) by optically tracking a reflective block marker on the holder of QUASAR® platform.[33] The total acquisition time for both scans was 8 min. The PET listmode data were saved for retrospective binning. CT images were acquired when the motion platform was not moving for attenuation correction with a CT technique used in our typical clinical PET/CT protocol (120 kVp, 120 mAs, pitch 1.375, 20 mm collimation, 2.5 mm slice thickness).

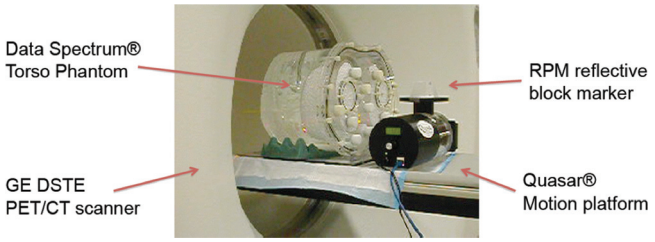

FIG. 1. Experiment setup of the phantom study. Note that the RPM block marker (white) was put on top of the motor of QUASAR platform (black part).

II.B. Patient data sets

Three wholebody PET/CT patient data sets with a total of eight visible lesions in the lung and abdomen regions were acquired with GE DSTE PET/CT scanner operating in 2D acquisition mode. Nuclear medicine physicians identified all lesions as potential tumors with focal FDG uptake. These data sets were selected to include localized lesions close to diagram. The motion signals of all three patients were regular without substantial long-term pattern change. The acquisition time for each bed position was 7 min. The patients were breathing freely during the acquisition. The patient motion was monitored and recorded by the RPM system, which records the anterior–posterior (AP) chest/abdomen displacement by optically tracking the reflective block marker on the patient chest/abdomen. The helical CT images used for attenuation correction were acquired with the same parameters as the phantom study at arbitrary breathing displacements during free breathing.

II.C. Generation of internal tumor respiratory signal

The process of generating an internal tumor motion signal is illustrated in Fig. 2. The proposed INTEX method is motivated by studies demonstrating that the external chest/abdomen anterior–posterior motion is well correlated with the internal tumor superior–inferior motion.[33,34] Based on the external motion signal acquired by the RPM system, we binned the PET listmode data for each study into five phase frames with equal counts and reconstructed each frame using OS-EM algorithm with two iterations and 28 subsets[35] and smoothed with an 8 mm Gaussian postreconstruction filter. Corrections for attenuation, scatter, random coincidences, deadtime, and detector efficiency were included in the reconstruction. The lesion in each reconstructed frame was segmented by a semi-automatic method[36] and the centroids of the segmented tumor were then determined. Only the superior–inferior direction component of the centroid was used in this study. We discuss the use of information in left–right and anterior–posterior directions in the Discussion section. The mean displacements of the external RPM signal that corresponds to each phase frame were determined. Then we compared the lesion centroid locations in the phase-gated images with the mean displacements of corresponding RPM

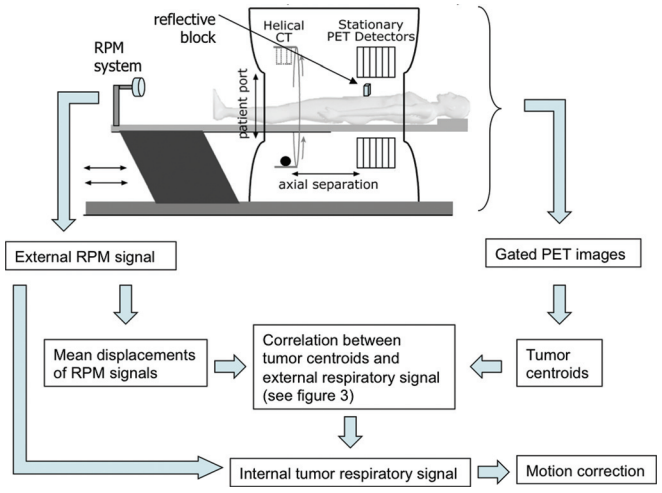

FIG. 2. The working flow of generating the internal tumor motion signal. The tumor centroids in superior–inferior direction in the phase-gated images and the corresponding mean displacements of external RPM signal are correlated. This relationship is then applied to the entire external motion signal to generate the internal tumor motion signal.

signals. We estimated the relationship between lesion centroids and RPM mean displacements with a linear function for all phantom and patient studies in this paper, and one patient example is shown in Fig. 3. This linear function was subsequently used to convert the original external RPM signal into an internal tumor motion signal in the superior–inferior direction with high temporal resolution.

II.D. Motion correction using internal tumor respiratory signals

For the bed position containing the lesion of each phantom and patient dataset, we binned the PET listmode data to sequential 1-second (1-s) dynamic frames. Each frame was precorrected for detector efficiency to avoid interpolating gaps caused by detector efficiency variations during registration. Thus, no correction for detector efficiency was performed during the final reconstruction. As illustrated in Fig. 4, according to the internal motion signal in the superior–

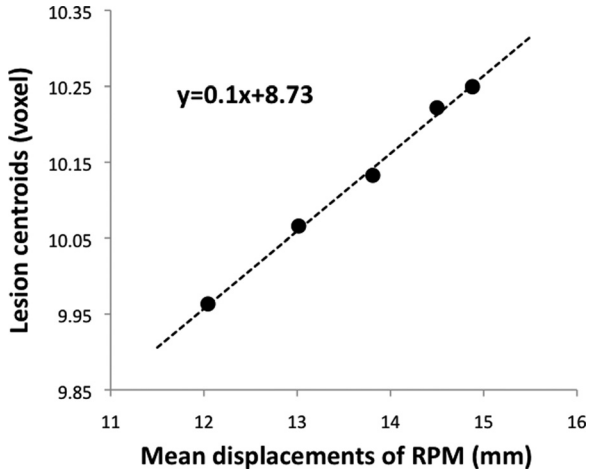

FIG. 3. A sample correlation of lesion centroids and RPM mean displacements derived from five-bin phase gating of a sample patient study. The five data points came from five gated images. A linear relationship was fitted.

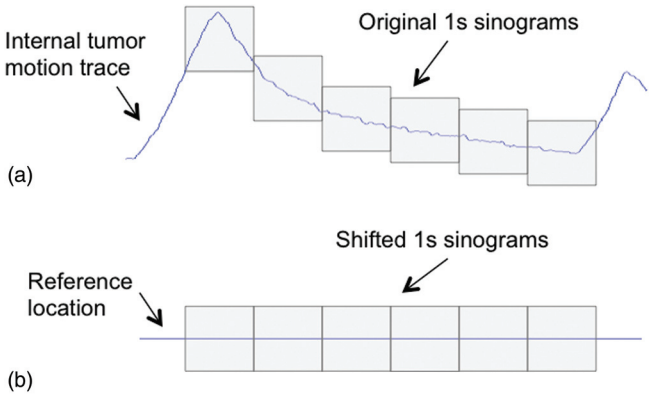

FIG. 4. Illustration of a portion of (a) precorrected and (b) postcorrected sinograms based on the knowledge of internal tumor motion information. Each box represents a 1-s sinogram and its vertical position corresponds to the tumor location before and after correction. The reference location was determined by methods in Sec. II E.

inferior direction of a given tumor (generated with the process in the previous section), each 1-s dynamic frame was axially registered to a reference location using linear interpolation. All the aligned frames were summed to generate a motion-corrected sinogram, which was subsequently reconstructed using OS-EM algorithm with corrections for attenuation, scatter, and random coincidence to form a motion-corrected PET image. The choice of reference frame was determined with a consideration for axially-aligned attenuation correction as described in the next section.

For comparison, five-bin phase-gated and ungated sinograms were generated and reconstructed with the same parameters in Sec. II C for the moving phantom and patient data. The stationary phantom data were also reconstructed as the gold standard "truth" for evaluation. To further compare the proposed INTEX method with a motion correction method that uses all detected events, we registered each image frame of five-bin phase gating to a reference frame according to the superior–inferior direction component of the lesion centroid in each gated image. Finally, all registered image frames were averaged to generate a final image. This method is referred as "Register and Average" in this study.

II.E. Matched attenuation correction with consistency condition

For each patient, the helical CT images for attenuation correction are mismatched with the PET images due to patient respiratory motion. To minimize the attenuation correction mis-match, the reference frame, to which other 1-s dynamic frames are shifted, was chosen based on the 2D Radon consistency conditions of the attenuation correction data. We have employed this method to perform automated alignment of PET and CT data for cardiac PET/CT and have used it for selecting matched CT and PET phases for FDG oncology imaging.[37,38]

In brief, PET data with accurate attenuation correction should meet the 2D Radon consistency conditions. These conditions state the moments of the projections through the

activity object are periodic with azimuthal angle. For example, the zero-order moment describes the property that the sum of the projection data for each view of a set of parallel-beam projections is a constant, independent of the projection angle. In this work, we applied the attenuation correction from the single helical CT to each of the five phase gated PET frames. The attenuation-corrected PET frame that best matches the first three moments of the 2D Radon consistency conditions was considered to have the best positional match with the attenuation map. This approach evaluates the Radon consistency condition in a global manner for the whole PET bed position image. Therefore, small local nonrigid distortions caused by respiratory motion and/or CT mismatch are not expected to have a negative impact of this approach. The mean displacement of this best-matched PET frame was used as the reference position for the subsequent axial shifts of all the 1-s frames.

II.F. Evaluations

The maximum lesion concentration in terms of MBq/cc was measured in the phantom study. For patient studies, the maximum standardized uptake value (SUVmax) of the lesion was measured for ungated images, five-bin phase-gated, Register and Average image, and INTEX images. For our proposed INTEX method, phase-gating, and Register and Average method, the lesion SUVmax change with respect to that of the ungated images were calculated as:

$$\Delta\text{SUVmax} = \frac{\text{SUV}_{\text{corrected}} - \text{SUV}_{\text{ungated}}}{\text{SUV}_{\text{ungated}}}, \quad (1)$$

where the $\text{SUV}_{\text{ungated}}$ denotes the lesion SUVmax measured from ungated images. $\text{SUV}_{\text{corrected}}$ denotes the lesion SUVmax measured from our proposed INTEX images, or the averaged lesion SUVmax across five phase-binned images, or the lesion SUVmax obtained from Register and Average method. We hypothesize that larger SUVmax increase correlates with less respiratory motion degradation and improved tracer quantification accuracy, if the methods being compared have the same image noise level.[6] However, this hypothesis does not apply for gated images as each five-bin gated frame contains only 20% of the detected events and the increased image noise leads to SUVmax overestimation.[18]

The lesion volume was measured using a semi-automatic segmentation method[36] for each image in the patient study. For motion-corrected images, the lesion volume change with respect to that of the ungated images were analyzed as:

$$\Delta\text{Volume} = \frac{\text{Volume}_{\text{corrected}} - \text{Volume}_{\text{ungated}}}{\text{Volume}_{\text{ungated}}}, \quad (2)$$

where the $\text{Volume}_{\text{ungated}}$ denotes the lesion volume measured from ungated images. $\text{Volume}_{\text{corrected}}$ denotes the lesion volume measured from our INTEX images, or the averaged lesion volume across five phase-binned images, or the lesion volume obtained from the Register and Average method.

III. RESULTS

Figure 5 shows images of the liver lesion in the phantom study with 16 mm motion amplitude. Compared to the stationary image, the ungated image appears visually blurred. The phase-gated images corrected for motion at the expense of higher image noise, which can lead to overestimation of SUVmax. Both the Register and Average method and the INTEX method corrected for the motion without increasing image noise. The INTEX method is visually closer to the truth image than the Register and Average method.

Figure 6 shows the quantitative analysis of different methods for lung and liver lesions in the phantom study with 16 and 11 mm motion amplitudes. For both amplitudes, the phase-gating method generally gave lower mean concentration compared to those of the stationary truth images with large variances across five bins, except for the lung lesion with 11 mm motion amplitude. Without increasing image noise, the Registration and Average method gave slightly underestimated tumor concentration. The proposed INTEX method nearly fully recovered the tracer concentration in each lesion for both motion amplitudes.

In patient study, the PET gates that have the best match with CT image are 5, 1, and 4 for patients 1–3, respectively. Figure 7 presents sample liver lesion images from a patient study. The proposed INTEX motion correction method led to higher lesion SUV and smaller lesion volume indicated by visual observation of the image. Compared to phase gating, both the Register and Average method and INTEX method led to improvement in tracer concentration and volume reduction, but with much lower image noise. This image noise was as low as in the ungated image, due to the utilization of all detected event without data rejection inherent in gating methods.

Table I summarizes the changes of tumor SUVmax and tumor volume for all the patients and lesions. We compared

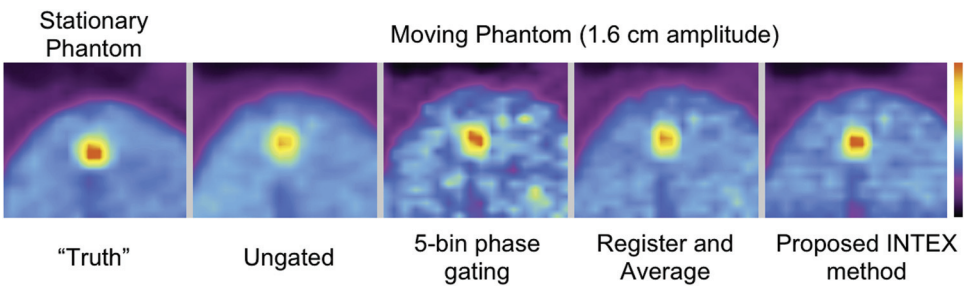

FIG. 5. Sample liver lesion images in the phantom study with different imaging methods. All images have matched color scale.

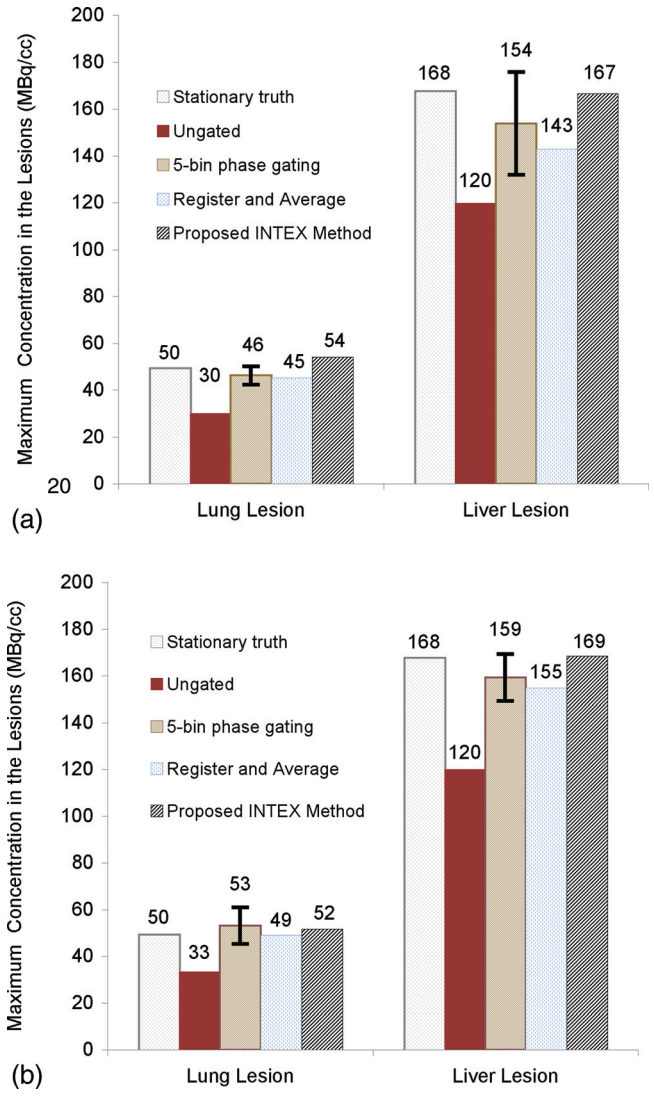

FIG. 6. Maximum tracer concentrations in lung and liver lesion in the phantom study for different methods with (a) 16 mm motion amplitude and (b) 11 mm motion amplitude. The maximum concentration values are shown above to each data point. For phase gating, the data are shown as means and standard deviations (indicated by error bar) across five phases. The proposed INTEX method effectively recovered the tracer concentration to the level of stationary "truth."

INTEX method to the Register and Average method as both utilized all detected events leading to same image noise level. The INTEX method led to 10.1% SUVmax increase and 17.0% volume decrease on average with standard deviations of 10.2 and 21.6%, respectively. The Register and Average method led to 9.5% SUVmax increase and 17.6% volume decrease on average with standard deviations of 5.8 and 20.7%, respectively. Lesion volumes were measured by methods in Ref. 36 from ungated images. Though the measured volumes are not accurate, it provides a rough idea of the lesion sizes in this study. The lesion motion amplitudes were determined as the largest superior–inferior centroid differences among five gated image frames. With intragate motion, this amplitude measurement is underestimated but provides a rough idea of motion amplitude.

IV. DISCUSSION

In this study, we proposed and evaluated a respiratory motion correction method for PET/CT using internal–external motion correlation. The derived internal–external motion correlations are used to align raw sinogram data, which is then reconstructed into a single image with respiratory motion of the tumors removed. The proposed INTEX method was specifically designed to improve quantification and delineation of known tumors in the lung and abdomen for assessing response to therapy and treatment planning. This method would not be appropriate for detection or staging studies, since the first step is to segment a known tumor and determine the centroids. This tumor and centroid information then undergoes the second-pass analysis described in this study.

Using all detected events, the images of the INTEX method have the same image noise level as that of the ungated images. Compared to other motion correction methods, such as respiratory-gating methods that include only a fraction of the detected events and yield higher image noise, the INTEX method corrects for respiratory motion without increasing the image noise. This is particularly important for tumor quantification, as we previously found that increased image noise alone can cause 9% tumor SUVmax overestimation on average across 31 tumors for five-bin phase gating.[18]

In the phantom study, five-bin phase gating led to underestimated tracer concentration on average, due to the intragate motion in each gated frame. This intragate motion comes from two contributions: (1) the finite period of time frames and (2) the long-term breathing pattern changes with baseline variation. The only exception of concentration underestimation in the phantom experiments was the study

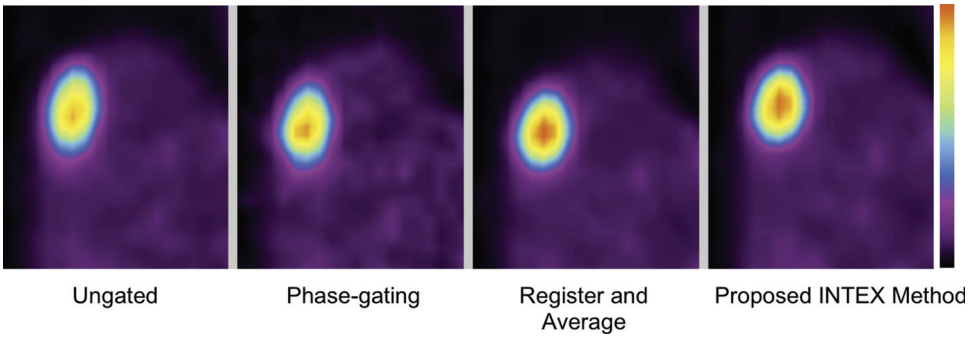

FIG. 7. Liver lesion in sample patient images generated with different methods. All images have matched color scale.

TABLE I. Changes of tumor SUVmax and volume compared to static ungated images for the Register and Average method and the proposed INTEX method for all patient lesions. Tumor volumes and motion amplitudes in the ungated images are shown.

	Tumor SUVmax changes		Tumor volume changes			
	Register and Average (%)	INTEX method (%)	Register and Average (%)	INTEX method (%)	Motion amplitude (mm)	Tumor volume (cc)
Patient 1 lesion 1	7.8	9.0	−10.0	−11.7	13.18	16
Patient 1 lesion 2	12.3	−4.0	−17.5	−8.4	8.12	11.3
Patient 2 lesion 1	5.3	8.1	14.7	−5.9	6.33	6.65
Patient 3 lesion 1	7.8	5.3	−6.5	−7.1	11.87	16.63
Patient 3 lesion 2	8.5	10.1	−19.0	−19.1	6.73	3.62
Patient 3 lesion 3	12.5	21.1	−28.1	−15.7	9.95	3.13
Patient 3 lesion 4	20.6	28.1	−62.4	−68.3	8.69	6.36
Patient 3 lesion 5	1.2	3.0	1.0	0.3	7.57	29.24
Mean ± standard deviation	9.5 ± 5.8	10.1 ± 10.2	−17.6 ± 20.7	−17.0 ± 21.6	9.06 ± 2.44	11.62 ± 8.81

of a lung lesion with 11 mm motion amplitude, where the overestimation may have come from increased image noise. The standard deviations were large, indicating nonuniform performance of each gated frame. Even though each gated frame contains less detected events and has higher image noise that can cause overestimation, the magnitude of intragate motion is generally large enough to cause underestimation of the tracer quantification. These two competing effects make prediction of the overall impact on quantification more complicated. The Register and Average method, which was derived from phase gating that contains intragate motion but used all detected events without increasing image noise, also led to tracer concentration underestimation. In contrast, the proposed INTEX method nearly fully recovered the tracer concentration to the level of the stationary "truth" images. Even though the current implementation of INTEX method is based on binned 1-s frames that still contain the first component of intragate motion discussed above, the INTEX method inherently eliminates the second component of intragate motion due to long-term baseline variations, which are present in phase-gating and the Register and Average method. Considering each phase-gated image represents the accumulation of many seconds (for example, a five-bin phase gating of a 5 min acquisition means each gate contains 1 min of information), intragate motion is larger than 1-s intraframe motion in the INTEX method. We expect that further improvement of the INTEX method with event-by-event motion correction discussed below will fully eliminate all the intraframe motion. Comparing the results of 11 and 16 mm motion amplitudes, the Register and Average method and phase gating resulted in less bias for smaller motion amplitude (11 mm) than for larger amplitude (16 mm). This is expected as larger motion amplitude lead to more intragate motion. However, the INTEX method effectively recovered the tracer concentration for both amplitudes, indicating that the performance of the INTEX method is less sensitive to motion amplitude. These phantom results with known truth demonstrated proof of concept of the proposed INTEX method.

For PET/CT patient studies, mismatched attenuation correction can cause tumor quantification errors, particularly with CT-based attenuation correction that can be acquired at an arbitrary breathing displacement when the patient is under free breathing during the acquisition.[39] The attenuation images of all patient data in this study were generated from helical CT scans, and there are potential attenuation correction errors due to positional mismatch. To account for mismatched attenuation correction, the INTEX method registered each 1-s sinogram to a reference frame. The reference frame was the one from the original five bin phase-gated PET data that best aligned with the helical CT image as determined by the Radon consistency conditions. Therefore, after summing all the registered sinograms, the summed sinogram is reconstructed with attenuation correction using a matched attenuation map. This leads to minimal attenuation correction errors. As shown in results, the best-matched gate is different for each patient, indicating that patient-dependent consistency check is necessary to match PET and CT data.

In patient study as shown in Table I, the proposed INTEX method led to higher SUVmax for six lesions out of eight compared to the Register and Average method. On average, the INTEX method and the Register and Average method provide similar improvement on SUVmax and volume estimation. Without the known truth, it is hard to tell which method has superior performance in this pilot study with such a small number of patients. However in the phantom study with known truth discussed above, we found that the proposed INTEX method offers superior performance. Further evaluation is needed in the future to fully investigate the benefit of the INTEX method in patient studies.

We demonstrated that the proposed INTEX method improves PET quantitative accuracy and volume estimation in this proof-of-concept study. There are two potential refinements: using listmode event-by-event positioning and fully 3D motion correction. For this preliminary study, we first binned the PET listmode data into multiple sequential sinograms whose duration is 1 s. Therefore, each 1-s sinogram contains a small amount of residual intraframe motion. Considering our approach has high temporal-resolution knowledge of the tumor motion (with same resolution as the external tracking device), we could virtually eliminate intraframe motion through

repositioning each listmode event to the reference frame during the listmode binning, instead of binning listmode data into multiple sinograms first and registering each of them. Listmode repositioning has been proposed for motion compensation in PET.[22] These methods differ from our proposed approach because the motion vectors are defined only for each gate. Therefore, these methods are susceptible to intragate motion. In this preliminary study, we showed that binning coarse 1-s sinogram leads to superior performance in tumor quantification and volume measurement. It is expected that further improvement can be achieved by using the listmode repositioning method in future work.

In this study, we implemented the INTEX method in the superior–inferior direction, which for lung and abdomen organs is roughly twice the magnitude of other directions on average.[40] We can extend this method in the left–right and anterior–posterior directions to achieve fully 3D correction for the respiratory motion. It is more intuitive to perform 3D correction in image space. This requires individually reconstructing each 1-s frame first, then registering, and then averaging. This is suboptimal primarily because of the computational demand of multiple image reconstructions for each frame. Therefore, we need to correct the motion in list-mode or sinogram space first. We could first convert the external RPM signal into three separate internal tumor motion signals in the superior–inferior, left–right, and anterior–posterior directions, respectively. To register the 1-s frames or to reposition listmode events, the motion vectors determined by internal motion traces in the image space need to be forward-projected onto the sinogram space to establish necessary motion information to guide the sinogram registration or listmode repositioning. The fully 3-dimensional (3D) motion-corrected sinograms could then be summed and reconstructed as described in this study. This work is currently under investigation. We expect further improvement can be achieved with fully 3D version of the proposed INTEX method and potentially all the tumor motion can be eliminated.

The accuracy of the proposed INTEX method relies on the correlation between internal tumor motion and external AP motion monitored by the RPM system. This correlation has been demonstrated in numerous studies.[33,34,41–43] However, these studies also indicated that a small fraction of patients whose tumor motion does not correlate well with the external motion monitoring systems. In these cases of poor internal–external correlation, the accuracy of the proposed INTEX method may be limited. This may explain the result of patient 1 lesion 2 in Table I, where the INTEX method caused negative SUVmax change compared to ungated image. To solve this potential challenge, estimating the internal tumor motion signal directly from PET data instead of converting from an external signal can be helpful. While PET data-driven motion estimation has been shown to be feasible,[44–49] there is still a major challenge for estimating the absolute tumor displacement information with sufficient temporal resolution, particularly for smaller lesions with low contrast.

The processing time of the INTEX method, as currently implemented, is in the order of hours, depending on the total acquisition time. The processing time is predominantly used to bin each 1-s sinograms. Implementation of the listmode event-by-event repositioning method will reduce the processing to several minutes. Also, since we are only interested in accurately quantifying and delineating a known tumor, both the interpolation and listmode repositioning methods can be performed only for the positions corresponding to a predefined volume-of-interest that contains the tumor. This would significantly speed up the computation process without degrading tumor quantification and delineation.

The internal–external correlation in this study was derived from five-bin phase gating, which is often used in clinical practice. By increasing the number of phase bins, more accurate correlation relationship may be achieved. However, with a larger number of respiratory phase bins, each gated image will be noisier. This increased image noise will negatively impact the centroid estimation from gated image. Therefore, the optimal number of gated bins to estimate internal–external correlation needs further investigation. It is expected that the optimal number depends on lesion size, motion amplitude, and image noise level, which is determined by factors such as patient weight, acquisition protocol, and reconstruction parameters.

It should be noted that, although the human body deforms nonrigidly during breathing, we assume the tumor moves rigidly. Therefore, while the tumor, which is the only tissue we are interested in quantifying here, will be arguably well registered, the rigid registration of 1-s sinograms in this study may lead to inaccuracies for the rest of body. The rigid registration may also affect the attenuation correction, as the PET and CT data may not be quite matched in other areas outside the tumor where attenuation ray sums across through the tumor as well as other remote regions. We do not expect this limitation will significantly change the conclusion of this study, because the local "self" attenuation of the tumors is the dominant effect.[50]

V. CONCLUSION

The proposed INTEX method determines the patient-specific relationship of internal tumor motion with external respiratory tracking information. This relationship allows the external tracking information to drive the repositioning of raw data to compensate for respiratory motion. Phantom and initial patient studies demonstrate that the proposed respiratory motion correction method improves quantification and delineation for known tumors in PET images.

ACKNOWLEDGMENTS

This work is funded by NIH grants R01-CA115870, K25-HL086713, and a research contract from GE Healthcare. We would like to thank Ravindra Manjeshwar from GE Global Research Center and Paul Keall from Stanford University for helpful discussions.

[a]Author to whom correspondence should be addressed. Electronic mail: chi.liu@yale.edu

[1]W. A. Weber, "Assessing tumor response to therapy," J. Nucl. Med. **50** (Suppl. 1) 1S–10S (2009).

[2]Y. E. Erdi, S. A. Nehmeh, T. Pan, A. Pevsner, K. E. Rosenzweig, G. Mageras, E. D. Yorke, H. Schoder, W. Hsiao, O. D. Squire, P. Vernon, J. B. Ashman, H. Mostafavi, S. M. Larson, and J. L. Humm, "The CT motion quantitation of lung lesions and its impact on PET-measured SUVs," J. Nucl. Med. **45**, 1287–1292 (2004).
[3]B. Thorndyke, E. Schreibmann, A. Koong, and L. Xing, "Reducing respiratory motion artifacts in positron emission tomography through retrospective stacking," Med. Phys. **33**, 2632–2641 (2006).
[4]S. A. Nehmeh and Y. E. Erdi, "Respiratory motion in positron emission tomography/computed tomography: A review," Semin. Nucl. Med. **38**, 167–176 (2008).
[5]T. Kawano, E. Ohtake, and T. Inoue, "Deep-inspiration breath-hold PET/CT of lung cancer: Maximum standardized uptake value analysis of 108 patients," J. Nucl. Med. **49**, 1223–1231 (2008).
[6]C. Liu, L. A. Pierce II, A. M. Alessio, and P. E. Kinahan, "The impact of respiratory motion on tumor quantification and delineation in static PET/CT imaging," Phys. Med. Biol. **54**, 7345–7362 (2009).
[7]A. F. Abdelnour, S. A. Nehmeh, T. Pan, J. L. Humm, P. Vernon, H. Schoder, K. E. Rosenzweig, G. S. Mageras, E. Yorke, S. M. Larson, and Y. E. Erdi, "Phase and amplitude binning for 4D-CT imaging," Phys. Med. Biol. **52**, 3515–3529 (2007).
[8]M. Dawood, F. Buther, N. Lang, O. Schober, and K. P. Schafers, "Respiratory gating in positron emission tomography: A quantitative comparison of different gating schemes," Med. Phys. **34**, 3067–3076 (2007).
[9]M. Guckenberger, M. Weininger, J. Wilbert, A. Richter, K. Baier, T. Krieger, B. Polat, and M. Flentje, "Influence of retrospective sorting on image quality in respiratory correlated computed tomography," Radiother. Oncol. **85**, 223–231 (2007).
[10]W. Lu, P. J. Parikh, J. P. Hubenschmidt, J. D. Bradley, and D. A. Low, "A comparison between amplitude sorting and phase-angle sorting using external respiratory measurement for 4D CT," Med. Phys. **33**, 2964–2974 (2006).
[11]S. A. Nehmeh, Y. E. Erdi, T. Pan, A. Pevsner, K. E. Rosenzweig, E. Yorke, G. S. Mageras, H. Schoder, P. Vernon, O. Squire, H. Mostafavi, S. M. Larson, and J. L. Humm, "Four-dimensional (4D) PET/CT imaging of the thorax," Med. Phys. **31**, 3179–3186 (2004).
[12]S. A. Nehmeh, Y. E. Erdi, T. Pan, E. Yorke, G. S. Mageras, K. E. Rosenzweig, H. Schoder, H. Mostafavi, O. Squire, A. Pevsner, S. M. Larson, and J. L. Humm, "Quantitation of respiratory motion during 4D-PET/CT acquisition," Med. Phys. **31**, 1333–1338 (2004).
[13]T. Pan, T. Y. Lee, E. Rietzel, and G. T. Chen, "4D-CT imaging of a volume influenced by respiratory motion on multi-slice CT," Med. Phys. **31**, 333–340 (2004).
[14]T. Pan, X. Sun, and D. Luo, "Improvement of the cine-CT based 4D-CT imaging," Med. Phys. **34**, 4499–4503 (2007).
[15]E. Rietzel, T. Pan, and G. T. Chen, "Four-dimensional computed tomography: Image formation and clinical protocol," Med. Phys. **32**, 874–889 (2005)
[16]N. Wink, C. Panknin, and T. D. Solberg, "Phase versus amplitude sorting of 4D-CT data," J. Appl. Clin. Med. Phys. **7**, 77–85 (2006).
[17]J. W. Wolthaus, M. van Herk, S. H. Muller, J. S. Belderbos, J. V. Lebesque, J. A. de Bois, M. M. Rossi, and E. M. Damen, "Fusion of respiration-correlated PET and CT scans: Correlated lung tumour motion in anatomical and functional scans," Phys. Med. Biol. **50**, 1569–1583 (2005).
[18]C. Liu, A. Alessio, L. Pierce, K. Thielemans, S. Wollenweber, A. Ganin, and P. Kinahan, "Quiescent period respiratory gating for PET/CT," Med. Phys. **37**, 5037–5043 (2010).
[19]T. Li, B. Thorndyke, E. Schreibmann, Y. Yang, and L. Xing, "Model-based image reconstruction for four-dimensional PET," Med. Phys. **33**, 1288–1298 (2006).
[20]R. Manjeshwar, X. Tao, E. Asma, and K. Thielemans, "Motion compensated image reconstruction of respiratory gated PET/CT," *3rd IEEE International Symposium on Biomedical Imaging* (Arlington, Virginia, 2006), pp. 674–677.
[21]F. Qiao, T. Pan, J. W. Clark, Jr., and O. R. Mawlawi, "A motion-incorporated reconstruction method for gated PET studies," Phys. Med. Biol. **51**, 3769–3783 (2006).
[22]F. Lamare, M. Ledesma, J. Carbayo, T. Cresson, G. Kontaxakis, A. Santos, C. C. Le Rest, A. J. Reader, and D. Visvikis, "List-mode-based reconstruction for respiratory motion correction in PET using non-rigid body transformations," Phys. Med. Biol. **52**, 5187–5204 (2007).
[23]F. Qiao, T. Pan, J. W. Clark, and O. R. Mawlawi, "Region of interest motion compensation for PET image reconstruction," Phys. Med. Biol. **52**, 2675–2689 (2007)
[24]F. Qiao, T. Pan, J. W. Clark, Jr., and O. Mawlawi, "Joint model of motion and anatomy for PET image reconstruction," Med. Phys. **34**, 4626–4639 (2007).
[25]M. Dawood, N. Lang, X. Jiang, and K. P. Schafers, "Lung motion correction on respiratory gated 3-D PET/CT images," IEEE Trans. Med. Imaging **25**, 476–485 (2006).
[26]T. Yamazaki, H. Ue, H. Haneishi, A. Hirayama, T. Sato, and S. Nawano, "An attenuation correction method for respiratory-gated PET/CT image," *IEEE Nuclear Science Symposium and Medical Imaging Conference Record* (San Diego, California, 2006), pp. 3292–3296.
[27]P. E. Kinahan, L. MacDonald, L. Ng, A. M. Alessio, W. P. Segars, B. M. Tsui, and S. Pathak, "Compensating for patient respiration in PET/CT imaging with the registered and summed phases (RASP) procedure," *IEEE International Symposium on Biomedical Imaging* (Arlington, Virginia, 2006), Vol. 2, p. 1104.
[28]P. E. Kinahan, S. Wollenweber, A. M. Alessio, S. Kohlmyer, L. MacDonald, T. K. Lewellen and A. Ganin, "Impact of respiration variability on respiratory gated whole-body PET/CT imaging," J. Nucl. Med. **48**, 196 (2007).
[29]G. S. Meirelles, Y. E. Erdi, S. A. Nehmeh, O. D. Squire, S. M. Larson, J. L. Humm, and H. Schoder, "Deep-inspiration breath-hold PET/CT: clinical findings with a new technique for detection and characterization of thoracic lesions," J. Nucl. Med. **48**, 712–719 (2007).
[30]S. A. Nehmeh, Y. E. Erdi, G. S. Meirelles, O. Squire, S. M. Larson, J. L. Humm, and H. Schoder, "Deep-inspiration breath-hold PET/CT of the thorax," J. Nucl. Med. **48**, 22–26 (2007).
[31]T. Torizuka, Y. Tanizaki, T. Kanno, M. Futatsubashi, E. Yoshikawa, H. Okada, and Y. Ouchi, "Single 20-second acquisition of deep-inspiration breath-hold PET/CT: Clinical feasibility for lung cancer," J. Nucl. Med. **50**, 1579–1584 (2009).
[32]S. Senan, D. De Ruysscher, P. Giraud, R. Mirimanoff, and V. Budach, "Literature-based recommendations for treatment planning and execution in high-dose radiotherapy for lung cancer," Radiother. Oncol. **71**, 139–146 (2004).
[33]A. S. Beddar, K. Kainz, T. M. Briere, Y. Tsunashima, T. Pan, K. Prado, R. Mohan, M. Gillin, and S. Krishnan, "Correlation between internal fiducial tumor motion and external marker motion for liver tumors imaged with 4D-CT," Int. J. Radiat. Oncol., Biol., Phys. **67**, 630–638 (2007).
[34]D. P. Gierga, J. Brewer, G. C. Sharp, M. Betke, C. G. Willett, and G. T. Chen, "The correlation between internal and external markers for abdominal tumors: implications for respiratory gating," Int. J. Radiat. Oncol., Biol., Phys. **61**, 1551–1558 (2005).
[35]H. M. Hudson and R. S. Larkin, "Accelerated image reconstruction using ordered subsets of projection data," IEEE Trans. Med. Imaging **13**, 601–609 (1994).
[36]T. B. Sebastian, R. Manjeshwar, T. J. Akhurst, and J. V. Miller, "Objective PET lesion segmentation using a spherical mean shift algorithm," *Med. Image Comput. Comput. Assist Interv. 2006*, Vol. 9, pp. 782–789.
[37]A. M. Alessio, P. E. Kinahan, K. M. Champley, and J. H. Caldwell, "Attenuation-emission alignment in cardiac PET/CT based on consistency conditions," Med. Phys. **37**, 1191–1200 (2010).
[38]A. M. Alessio, S. Kohlmyer, and P. E. Kinahan, "Consistency driven respiratory Phase alignment and motion compensation in PET/CT," *IEEE Nuclear Science Symposium and Medical Imaging Conference Record* (Honolulu, Hawaii, 2007), Vol. 4, pp. 3115–3119.
[39]P. E. Kinahan, B. H. Hasegawa, and T. Beyer, "X-ray-based attenuation correction for positron emission tomography/computed tomography scanners," Semin. Nucl. Med. **33**, 166–179 (2003).
[40]D. P. Gierga, G. T. Chen, J. H. Kung, M. Betke, J. Lombardi, and C. G. Willett, "Quantification of respiration-induced abdominal tumor motion and its impact on IMRT dose distributions," Int. J. Radiat. Oncol., Biol., Phys. **58**, 1584–1595 (2004).
[41]J. D. Hoisak, K. E. Sixel, R. Tirona, P. C. Cheung, and J. P. Pignol, "Correlation of lung tumor motion with external surrogate indicators of respiration," Int. J. Radiat. Oncol., Biol., Phys. **60**, 1298–1306 (2004).
[42]D. Ionascu, S. B. Jiang, S. Nishioka, H. Shirato, and R. I. Berbeco, "Internal–external correlation investigations of respiratory induced motion of lung tumors," Med. Phys. **34**, 3893–3903 (2007).
[43]Y. Seppenwoolde, H. Shirato, K. Kitamura, S. Shimizu, M. van Herk, J. V. Lebesque, and K. Miyasaka, "Precise and real-time measurement of 3D tumor motion in lung due to breathing and heartbeat, measured during radiotherapy," Int. J. Radiat. Oncol., Biol., Phys. **53**, 822–834 (2002).

[44]R. A. Bundschuh, A. Martinez-Moeller, M. Essler, M. J. Martinez, S. G. Nekolla, S. I. Ziegler, and M. Schwaiger, "Postacquisition detection of tumor motion in the lung and upper abdomen using list-mode PET data: a feasibility study," J. Nucl. Med. **48**, 758–763 (2007).
[45]F. Buther, M. Dawood, L. Stegger, F. Wubbeling, M. Schafers, O. Schober, and K. P. Schafers, "List mode-driven cardiac and respiratory gating in PET," J. Nucl. Med. **50**, 674–681 (2009).
[46]A. L. Kesner, R. A. Bundschuh, N. C. Detorie, M. Dahlbom, S. I. Ziegler, J. Czernin, and D. H. Silverman, "Respiratory gated PET derived in a fully automated manner from raw PET data," IEEE Trans. Nucl. Sci. **56**, 677–686 (2009).
[47]G. J. Klein, B. W. Reutter, E. H. Botvinick, T. F. Budinger, and R. H. Huesman, "Fine-scale motion detection using intrinsic list mode PET information," *IEEE Workshop on Mathematical Methods in Biomedical Image Analysis* (Kauai, Hawaii, 2001), pp. 71–78.
[48]P. J. Schleyer, M. J. O'Doherty, S. F. Barrington, and P. K. Marsden, "Retrospective data-driven respiratory gating for PET/CT," Phys. Med. Biol. **54**, 1935–1950 (2009).
[49]D. Visvikis, O. Barret, T. D. Fryer, A. Turzo, F. Lamare, C. Cheze Le Rest, and Y. Bizais, "A posteriori respiratory motion gating of dynamic PET images," *IEEE Nuclear Science Symposium and Medical Imaging Conference Record* (Portland, Oregon, 2003), Vol. 5, pp. 3276–3280.
[50]C. Bai, P. E. Kinahan, D. Brasse, C. Comtat, D. W. Townsend, C. C. Meltzer, V. Villemagne, M. Charron, and M. Defrise, "An analytic study of the effects of attenuation on tumor detection in whole-body PET oncology imaging," J. Nucl. Med. **44**, 1855–1861 (2003).